LIP-STUDENTS-20-03

Exploring the fast evolution of quark gluon plasma

Ema Mendes[1,a] and Marcelo Gonçalves[2,b]

[1] *Faculdade de Ciências da Universidade de Lisboa, Portugal*
[2] *Instituto Superior Técnico, Lisboa, Portugal*

Project supervisor: L. Apolinário, A. Cordeiro

October 2020

Abstract. The formation of Quark Gluon Plasma (QGP) and the phenomena of jet quenching in heavy-ion collisions have been confirmed experimentally over the past decade. In this paper we show results from simulated interactions between jets and the QGP medium formed in the collision, using a jet quenching Monte Carlo event-generator: JEWEL. Focusing on Z+jet events, we investigate how the jet energy loss distribution changes with the QGP parameters that define its temperature evolution. In particular, we check its dependence on the initial temperature T_i, initialization time τ_0, and evolution profile of the medium. We found that p_T^{jet}/p_T^Z is, by construction, quite sensitive to these parameters, but the fluctuations are roughly constant along the different changes. In order to isolate the effects in the fluctuations of the momentum of the jet discarding medium-induced energy loss processes we further analyzed the distribution of the ratio $p_T^{jet}/ < p_T^{jet} >$. Our results seem to indicate that this distribution enhances the fluctuations seen across the different setups. In addition, we found a significant discrimination between pp and $PbPb$, independently of the medium temperature. Future work along this direction may help to understand the puzzling observations on $PbPb$ and high multiplicity pp.

Keywords: LHC, heavy ions, hard probe, jets, jet quenching, JEWEL, Bjorken Expansion Model

1 Introduction

1.1 Quark Gluon Plasma (QGP)

Quantum chromodynamics (QCD) is one piece of the modern theory of particle physics called the Standard Model. The QCD theory is based on the color property of gluons, the carriers of the strong force, which can interact with each other. Furthermore, the coupling strength increases with the distance between particles in opposition to Quantum Eletrodynamics (QED).

QCD has two emerging properties that are unique with respect to other SM theories: Asymptotic freedom and Confinement. The first is characterised by a weak interaction between quarks and gluons, allowing to represent a QCD system as a group of asymptotically free particles. In this regime, that occurs when the energy of the interaction is large, analytical perturbative methods provide accurate physical predictions. Although of limited scope, this approach delivers several results that are of interest to other SM physics studies (e.g: BSM research). In the opposing limit (low energy) Color confinement is responsible for binding quarks and gluons inside hadrons (final state composite particle). The mechanism of confinement is still to be well understood analytically, but several efforts, in particular from lattice QCD calculations, are being studied to understand this phenomenon from first principles.

The richness of QCD lies also in its temperature/density phase space (see Fig.1). *Normal* hadronic matter, where quarks and gluons are confined into hadrons, lies in the low density/temperature corner. However, other states of matter are expected as we increase density and/or temperature. In particular, at very high temperatures we expect the production of a new state of matter, known as the Quark-Gluon Plasma (QGP)[1].

This state of matter is believed to have filled the entire universe shortly after the Big Bang, being, as such, of interest not only in Particle Physics, but also for Cosmology related studies! Currently it can be produced in the laboratory through relativistic heavy ion collisions, such as gold or lead (Pb) nuclei, where it is possible to reach very high temperatures and densities, fig.1.

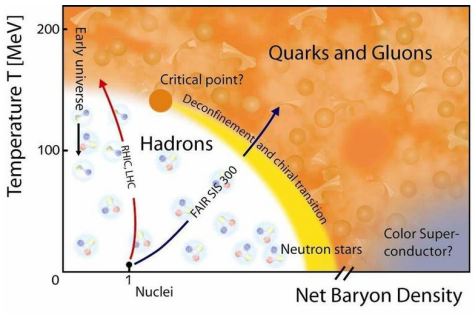

Figure 1. Phase diagram of QCD. The phase boundary between confined hadronic matter and the quark gluon plasma is illustrated by the yellow band. Analog to the phase diagram of water, a critical point exists, beyond which the phase boundary disappears and the transition occurs continuously.[2]

The result of a heavy-ion collision is the QGP production that will shortly start to expand and hadronize into colorless bound states (see schematic view of a heavy-ion collision evolution in fig.2). The QGP phase is extremely short, of the order on the *fm/c*, i.e., yoctoseconds scale ($\simeq 10^{-24}$ s).

[a] e-mail: emamendes2000@gmail.com
[b] e-mail: marcelo.goncalves@tecnico.ulisboa.pt

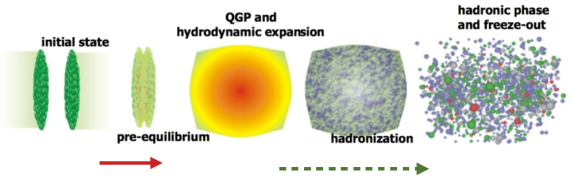

Figure 2. Schematic evolution of the QGP through its different stages during an heavy ion collision. [3]

With such short lifetime it is impossible to probe this medium externally, so we must find other ways to study its properties, in particular we must use a product that arises from a head-on collision between two high-momentum partons of the two incoming nuclei. These objects are known generically as Hard Probes, and they will be the focus of this work.

1.2 Hard Probes and Jets

In particle physics we are more interested in describing the phenomena based on its microscopic interactions among the elementary constituents of matter.

As explained in the previous section, our focus will be in internal probes. We must distinguish two different types of probes depending on their energy scale: Soft probes and Hard probes. Soft probes are the result of the QGP evolution and, therefore, are sensitive to the macroscopic and collective properties of QGP. However they cannot be described under the perturbative QCD formulation because of their low energy and momentum. So we will redirect our attention onto hard probes. Since they are high momentum and very energetic particles, they are within the perturbative regime of QCD, meaning we have a well-formulated theory to describe their behaviour and interactions, at least in vacuum, up to the hadronization scale. In the presence of a medium, the energy scale of the interaction between probe and the QGP lies at the borderline where perturbative methods can be applied. In what follows, we will use a model that assumes a perturbative description for the hard probes evolution and its interaction with the plasma.

One of these hard probes are jets. They are fundamental to QCD and are created over the radiation of quarks and gluons (as a way to loose energy and become bounded with each other). They are, by definition, composed of final state particles that have originated under the same high momentum parton produced in a hard scattering within the collision.

In pp (proton-proton) collisions they are very easy to identify but in Pb-Pb collisions, some jets can be thermalized by the medium and never reach our detectors, signaling the presence of the QGP. Obviously, the further a jet has to travel through the dense fireball of a heavy-ion collision – 30 to 50 times as dense as an ordinary nucleus – the more energy it looses. The jet will pass through the medium and often will not be completely absorbed by the surrounding quarks and gluons in the QGP. The degree of modifications that the jet will experience by interacting with the medium - a process usually known as jet quenching, reveal what's inside the fireball and thus the properties of the QGP, that we will study. [4]. Jet quenching phenomena includes energy loss processes, modifications to the jets' orientation, directionality, composition, and how they transfer energy and momentum to the medium.

2 Goal and Methodology

In the past decade the ALICE, ATLAS and CMS programs at CERN's Large Hadron Collider (LHC) have confirmed the phenomenon of jet quenching in heavy-ion collisions. The large energy reached in collisions, in LHC, push measurements to much higher jet energies that are accessible at RHIC (Relativistic Heavy Ion Collision), allowing new and more detailed characterization of the quark-gluon plasma. Theoretical understanding of these measurements is very challenging however, and is one of the most important problems in quantum chromodynamics today.

The time interval between the QGP's initial formation and final hadronization is very short. Consequently in Experimental Physics we only have access to the final product of the collision and the data collected has a lot of information that needs to be carefully analised and deconstructed. From the final picture, one must deduce and separate the various stages of QGP that the particles have been exposed to. Our ultimate goal with the project this paper introduces is to try and infer what happened during the various stages of QGP.

We made use of a Monte Carlo event-generator, named *JEWEL*[5], that simulated not only the particle collisions but also the effects of the propagation of the jet in the QGP medium. The program embodies an energy-loss based model, meaning it can replicate the effect of jet quenching that appears from heavy ions collisions, and allows the user to change some medium-parameters used during the simulation. In particular, the user can change:

- τ_0 : initial time. This is the time the QGP takes to complete its formation, where the temperature rises very quickly until reaching its maximum value. It is also the time needed for the QGP medium to reach its equilibrium phase, where the Bjorken Expansion Model can thereafter be applied.

- T_i : initial temperature of the QGP when it reaches a thermal equilibrium, being the maximum value in the temperature profile (fig. 3).

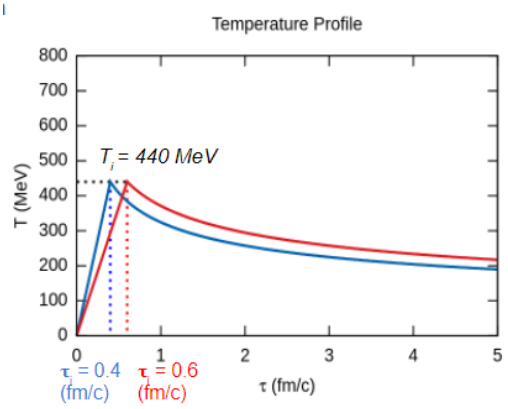

Figure 3. Medium temperature profile curve as a function of time, for two different initial time values.

In *JEWEL* the initial temperature growth occurs linearly. After the initial time, the medium follows a *Bjorken expansion*[3, 5], meaning temperature decreases over time following a power law, as follows:

$$T = \begin{cases} T_i \dfrac{\tau}{\tau_0} & \tau < \tau_0 \\ T_i \left(\dfrac{\tau}{\tau_0}\right)^{-\frac{1}{3}} & \tau \geq \tau_0 \end{cases} \quad (1)$$

While this evolution is fixed, we also change it directly in the program to account for a different initial evolution (plateau, see section 3.4) and different Bjorken powers (see section 3.2).

Our case of study is the channel *Boson(Z) + Jet*, see fig. 4, that are produced in the collision. The jet initiating parton will interact with the QGP thus loosing energy along the way. The Z boson, being a colourless particle, won't interact with the medium and because it is a product of the initial collision it will provide us with information about the initial energy of the jet. Due to energy-momentum conservation in the transverse plane at high energies, which is our case, in the hard scattering the 2 outgoing particles (the boson and a parton) will have precisely the same momentum-energy. Hence this channel has the advantage to have a good proxy for the original p_t (transverse momentum) or energy of the parton that originated the jet.

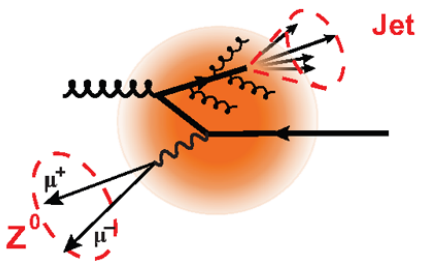

Figure 4. Schematic of the jet+Z set-up used during the simulation.

In our study we used JEWEL 2.1.0 and we simulated 1M hadronic events for each medium configuration. We selected the Z+jet event mode, forcing the Z-boson to decay into muons. On the reconstruction level, we first select the two hardest muons with a transverse momentum $p_{T,muon} > 10$ GeV and pseudo-rapidity $|\eta_{muon}| < 2.1$. The cluster made of these two muons is required to have a mass $m^{boson} \in [70; 110]$ GeV and a $p_T^{boson} > 60$ GeV. The remaining particles are clustered with the anti-k_T algorithm with a radius of $R = 0.5$ (unless noted otherwise). The final selected jet will be the hardest with a $p_T^{jet} > 30$ GeV and azimuthal angle with respect to the Z direction constrained to be $\Delta\phi > 7\pi/8$.

Later, we then looked at the average energy fraction distribution - the distribution of the p_T imbalance, $X_J^Z := p_T^{jet}/p_T^{boson}$, as it is a direct measure (an observable) of a well-calibrated jet energy loss[6]. In this case, we also looked at the fluctuations (the width of the distribution), to find out if they are sensitive to the initial time and to understand how a change in the QGP evolution can affect this distribution (and others).

By construction, the mean value of X_J^Z will change with all modifications in the QGP parameters (fig. 6) as they will reflect different magnitudes of medium-induced energy loss processes. Having more input parameters than experimental constrains, there is an additional freedom to tune the QGP characteristics as provided by each theoretical model (we know that we can find a certain combination of these simulation parameters that will give us the same result). By normalizing this distribution over its mean value we can discard this influence and focus only on the fluctuations. For such we also studied the ratio $p_T^{jet} / < p_T^{jet} >$ (fig. 7).

3 Results

We will now proceed to present the results obtained for each change on the QGP parameters and analyze the corresponding modifications of the transverse momentum ratio between the jet and the Z boson - X_J^Z - and also between the jet and its mean value - $p_T^{jet} / < p_T^{jet} >$ as follows.

3.1 Initial Temperature - T_i

As an example of the X_J^Z distribution, in fig.5 we have 2 histograms, one for a given initial temperature, T_i, of 220 Mev in red and another for a pp collision in blue. The red curve is flatter (more fluctuations) and its mean value is lower than that of the blue curve that is centered around 1, thus revealing additional energy loss processes expected from jet quenching effects. Our goal now is to understand how this distribution changes when we select different medium configurations.

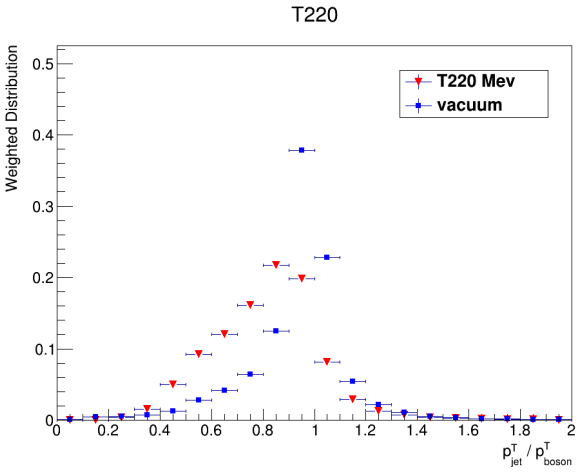

Figure 5. X_j^Z normalized distribution for a temperature of 220 Mev (red) and the same distribution for the pp collision (blue).

Starting with the change of the initial temperature of the QGP, the first results regarding the X_J^Z mean value (a) and fluctuations (b) can be found in fig.6. In the x-axis, we show the considered values of T_i varying from 220 Mev to a maximum of 550 Mev (the point at 0 Mev is a reference for the pp collision). The evolution of the X_J^Z distribution with temperature is shown for 2 different jet radius, R= 0.5 in blue and R= 1.0 in green.

We can verify a decrease in the average value of X_J^Z with the increase of the initial temperature. This comes as no surprise since we expect to have more energy loss in the jet the higher the temperature of the medium is.

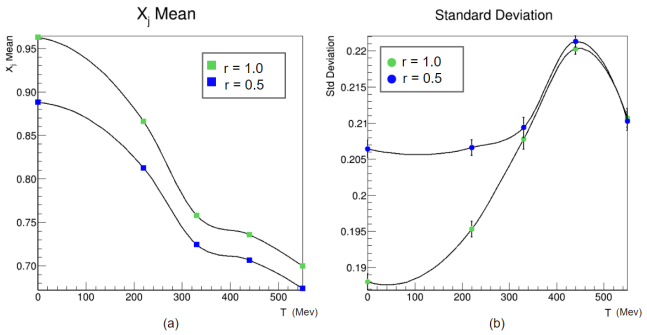

Figure 6. (a) X_j^Z mean values for 2 different jet radius, $r = 0.5$ and $r = 1.0$, as a function of T_i. (b) X_j^Z standard deviation for the same 2 different jet radius as a function of T_i.

The previous plot allows a comparison between two different jet radii. Apart from an obvious upward shift - as expected, the larger the jet radius, the more similar to pp collision we should be as we recover some of the jet energy - these results seem to be consistent for the two jet radius. In fig. 6-(b) where we have a plot regarding the fluctuations, in particular the standard deviation, once more the corresponding fluctuations seem to follow the same trend, especially for higher temperatures. For low temperatures, the higher the jet radius the higher the fluctuations are (at high temperatures this effect isn't so noticeable). At low temperatures, we approach pp results. By increasing the jet radius, we also recover most of the particles modified by the QGP interactions. As such, small fluctuations induced by the probabilistic interaction of the parton shower with the QGP constituents, will be more visible in a larger radius jets.

In figure 7 we can have a look at the shape of the distribution of the ratio $p_T^{jet} / < p_T^{jet} >$ for a given initial temperature, T_i, of 220 Mev (red) and the same distribution but for the case of the pp collision (blue). This distribution is also interesting to be taken into account in this study as, by definition, it will be less sensitive to the average energy loss. As it can be shown from 7, the average values of both distributions are now more similar (shift less visible), when compared to the figure 6. Nonetheless, we continue to see the overall broadening effects.

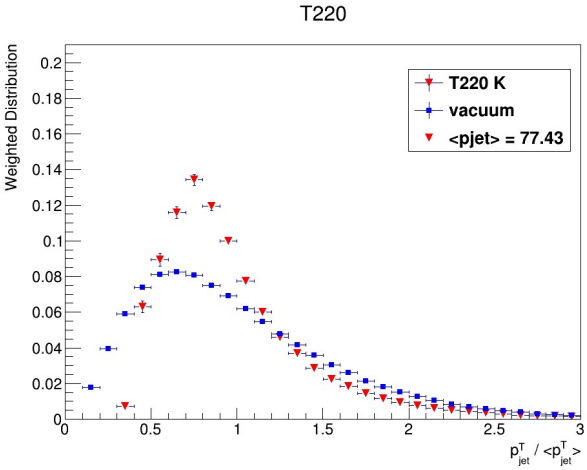

Figure 7. X_j^Z normalized distribution for a temperature of 220 Mev (red) and the same distribution for the pp collision (blue).

What follows now is a comparison regarding the effect of the change of T_i in the distribution of our two ratios - X_j^Z and $p_T^{jet} / < p_T^{jet} >$ - for same jet radius R = 0.5, as shown in fig. 8. On the x-axis we have T_i ranging once again between 220 Mev and 550 Mev and on the y-axis is the mean value (fig.6-(a)) and the fluctuations (fig.6-(b)) of the X_j^Z in blue and the $p_T^{jet} / < p_T^{jet} >$ in green.

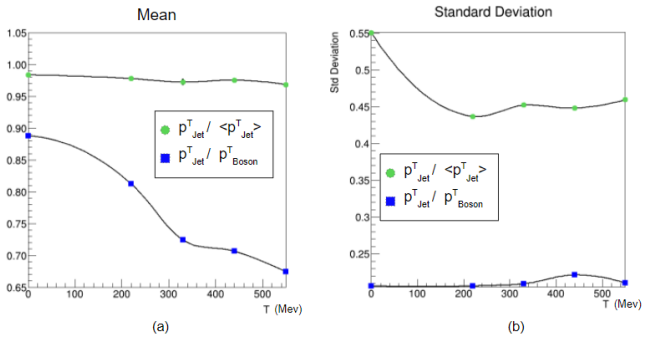

Figure 8. (a) X_j^Z and $p_T^{jet} / < p_T^{jet} >$ mean values as a function of T_i. (b) X_j^Z and $p_T^{jet} / < p_T^{jet} >$ standard deviation as a function of T_i.

As previously stated the ratio $p_T^{jet} / < p_T^{jet} >$ is almost insensitive to the energy loss, ~ 1. On the other hand in the fluctuations, fig.8-(b), while we continue to see a relatively small change with the medium temperature, there is a clear difference between pp and Pb-Pb collisions. This could potentially help to discriminate between "quenched" and "unquenched" jets independently of medium temperature and will be left for future studies.

On another note the $p_T^{jet} / < p_T^{jet} >$ ratio gives information about the final momentum of the jet discarding the average energy loss due to jet-medium interactions. The greater the interactions with the medium the more the left side of this distribution shifts to lower p_T values, thus increasing the standard deviation that now signals energy loss fluctuations from the jet development within the QGP. We will explore this feature in the following sections to understand if we can amplify possible shifts depending on the input medium parameters.

3.2 Bjorken Power

We will now describe our results obtained by changing the shape of the QGP medium using the jet radius $R = 0.5$. As stated before, in our simulation the temperature profile of the medium after its formation follows a power law, according to the expression (see equation 1):

$$T = T_i \left(\frac{\tau}{\tau_0} \right)^{-\frac{x}{3}} \tag{2}$$

where we decided to introduce a variable x in the exponent.

In the next plot we have the X_j^Z mean graph (fig.9-(a)) and fluctuations (fig.9-(b)) as a function of the temperature power law exponent, where x in equation (2) takes the values 0.5, 1, 2, and 3.

The results show that for a faster decreasing temperature there is less energy loss. It makes sense that in a medium that retains its temperature for longer the jet loses more energy. Nonetheless, the standard deviation, fig.9-(b), appears to be almost unchanged, when changing the temperature profile of the medium.

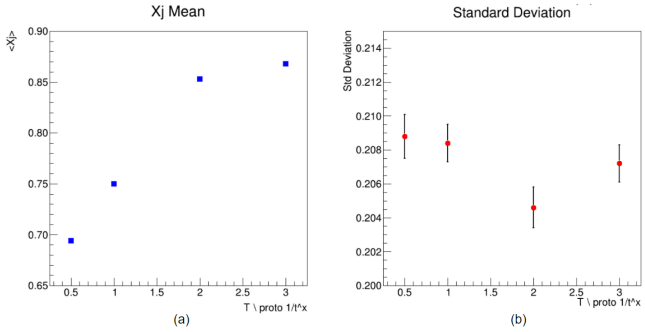

Figure 9. (a) X_j^Z mean values as a function of the power law exponent. (b) X_j^Z standard deviation as a function of the power law exponent.

For the $p_T^{jet} / < p_T^{jet} >$ ratio, fig.10 shows the fluctuations as a function of the temperature power law exponent in the x axis (we avoided including the average value as we already know that is compatible with 1). In this variable, fluctuations for a faster decreasing temperature profile seem to get closer to the pp collision reference. There is a maximum deviation in the fluctuations of 6.3% opposed to 1.1% that is possible to obtain from the X_j^Z. Even though the difference in fluctuations is not that large ($< 10\%$), it indicates that this distribution has more sensitivity to changes in the medium parameters. Still, this change will only affect the final development of the jet, where some of its fragmentation pattern is already constrained. In the next section, we will investigate how a change in the initial time of the medium can be potentially signaled on this distribution.

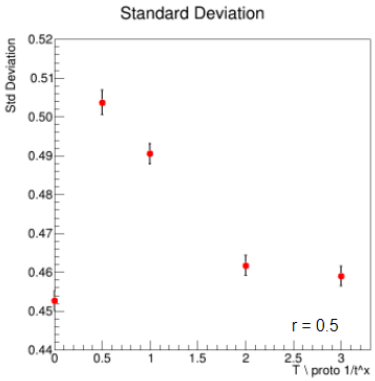

Figure 10. $p_T^{jet} / < p_T^{jet} >$ standard deviation as a function of the power law exponent for a radius jet $r = 0.5$.

3.3 Initial Time - τ_0

The effects of changing τ_0 in the energy loss of the jet (X_j^Z) are shown in the next figure. In fig.11, we show the X_j^Z mean value (a) and standard deviation (b) as a function of the following initial times: 0.2 fm, 0.4 fm and 0.6 fm.

With the increase of initial time we can clearly see an increase of the energy lost by the jet. That is expected since by choosing a later initial time there will be more particles in the jet to interact with the QGP at the moment its density is higher. Hence the larger probability will the jet have to lose some energy. The deviations in the fluctuations of X_j^Z continue to be small (3.6%).

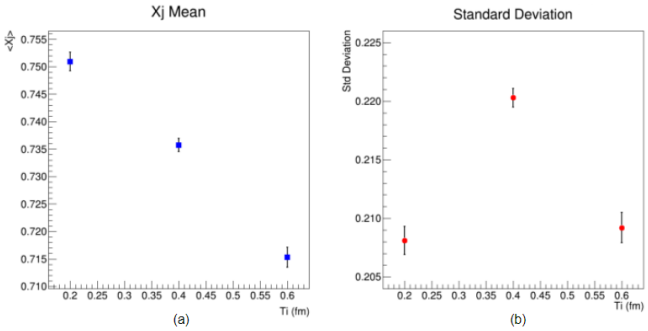

Figure 11. (a) X_j^Z mean values as a function of τ_i. (b) X_j^Z standard deviation as a function of τ_i.

The next graph, fig.12, concerns the $p_T^{jet} / < p_T^{jet} >$ ratio and the y-axis is the standard deviation. On the x-axis we have τ_i, assuming the values 0.2 fm, 0.4 fm and 0.6 fm once again.

We can observe that changing the initial time does not have an effect on the fluctuations, despite the fact it has an impact on the loss of momentum of the jet aforementioned.

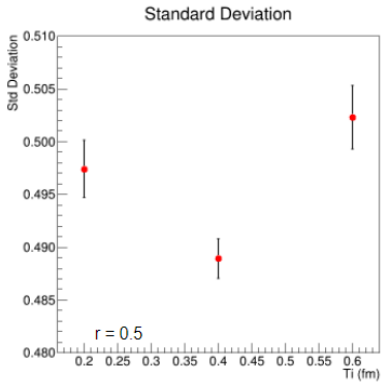

Figure 12. $p_T^{jet} / < p_T^{jet} >$ standard deviation as a function of τ_i.

Taking into account the results from the previous section, the fact that we do not see an effect on this observable might indicate that there is an interplay between a delayed QGP that reach its maximum density at a later time, and the status of development of the parton shower. Overall, these effects seem to cancel on the final distribution. In order to isolate them, we decided to change directly in the code the settings regarding the evolution of the QGP before τ_0, in other words, the initial temperature profile of the medium.

3.4 Initial QGP density evolution

According to the previous results we became interested in understanding the real effect the initial moments before the formation of the QGP have in the jet development, so we decided to try several different initial temperature profiles and study the fluctuations of the $p_T^{jet} / < p_T^{jet} >$ distribution, fig.13-(b), using as a reference the pp collision.

We used several different profiles that affect the QGP evolution from $\tau = 0$ up to $\tau = \tau_0$ (first branch of equation (1)). These are summarized in the following table:

Label	Description
pp	No QGP
$T = T_i/3$	Constant Initial temperature set at $T = T_i/3$, where T_i is the maximum QGP temperature
$T = T_i/2$	Constant Initial temperature set at $T = T_i/2$, where T_i is the maximum QGP temperature
$T = T_i$	Constant Initial temperature set at $T = T_i$, where T_i is the maximum QGP temperature
$T = T^3$	Growth of the QGP temperature that goes as $T = T_i \left(\frac{\tau}{\tau_i}\right)^3$
linear	Linear growth of the QGP (default parameterization within JEWEL)

Table 1. List of initial QGP density evolution input parameters that summarize the different initial shapes of the temperature profile studied.

We gathered the results of the mean value of the distribution (fig.13-(a)) and its standard deviation (fig.13-(b)) as a function of these different initial temperature curves.

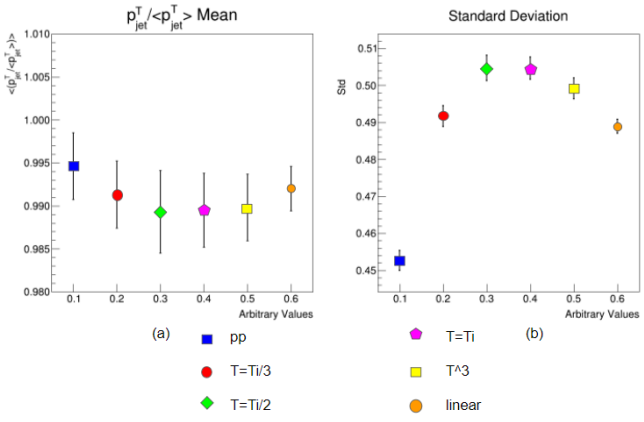

Figure 13. (a) $p_T^{jet} / < p_T^{jet} >$ mean values for different shapes of the initial temperature profile made by changing JEWEL simulation parameters. (b) $p_T^{jet} / < p_T^{jet} >$ standard deviation for the respective initial temperature profiles. Below there is a label of the points regarding the different initial temperature profile function simulated.

By order in the graph we have an initial temperature profile that is constant at $T = T_i/3$, $T = T_i/2$ and $T = T_i$. The next point is relative to a temperature profile that follows a power law to the third and finally a linear increase, the pre-defined option within JEWEL.

The default JEWEL initial time of 0.4 fm was used to keep the evolution of the QGP after this time fixed across the configurations.

Note that the plateau used needed to be above a certain critical temperature of formation of the medium, because if not, the simulation wouldn't produce the effects of energy loss. As such we were not able to test the extreme scenario where there isn't jet quenching before the initial time, τ_i, a case study that seems to be preferred in other jet quenching studies [7].

We included the mean value of the distribution for completeness, but, as expected, the changes are negligible (fig. 13). We can verify the fluctuations have a maximum deviation of 11.5% between pp and Pb-Pb and of around 3.3% between the Pb-Pb themselves. Although not too prominent there seems to be some discrimination to distinguish extreme scenarios on the initial QGP temperature evolution. This fluctuations might be enhanced if instead we choose $\tau_i = 0.6$ fm, the preferred value that comes from other jet quenching studies. Future work to understand how to maximize this effect within educated QGP parameters will be left for a future study.

4 Conclusions

Possibly the most important note from our results is that we may be able to discriminate between quenched and unquenched jets "independently of the temperature", that means we can tune the average value and look at the fluctuations, where they will show a sizable difference between pp and Pb-Pb. Of course, it'll need to be further checked. The next step would be to check if this same difference remains in light systems, low temperatures or even shorter media.

There seems to be some discrimination between shapes regarding the initial time, early and final stages of the medium. We find that if we delayed the QGP evolution, the fluctuations on $p_T^{jet} / < p_T^{jet} >$ will be constant across such modifications. Instead, by looking to changes specifically made only at initial or later times, this distribution shows more discrimination between the different configurations when comparing to the experimental measured distribution X_j^Z. As such, there is a cancellation of effects between the initial and final development of the jet when travelling through the QGP. This will need to be further studied in the future.

In addition, the difference in the fluctuations through the several configurations was limited to $1 - 10\%$. However, this study was very conservative as we could not explore the preferred QGP evolution scenario that is withdrawn from other jet quenching studies: absence of quenching effects up to τ_0. Together with the fact that we restricted ourselves to the default JEWEL parameters for $\tau_0 = 0.4$ fm, we believe that this analysis might be promising to understand how can we withdraw time differential information from the QGP by using jets. The next step would be to understand how to maximize the fluctuations for more realistic QGP evolution scenarios.

Acknowledgements

Thanks to Liliana Apolinário and André Cordeiro for being excellent supervisors, for being so reliable and always open to answer our questions and providing frequent feedback on our results. A big thank you to LIP for providing a fun and fulfilling internship (despite the current peculiar situation) and giving us the opportunity to become a researcher for a summer.

References

[1] W. Busza, K. Rajagopal, W. van der Schee, Ann. Rev. Nucl. Part. Sci. **68**, 339 (2018), 1802.04801

[2] G. Aarts, Journal of Physics: Conference Series **706** (2015)

[3] A.K. Chaudhuri, pp. 7–1 to 7–60 (2014)

[4] *Heavy ions and quark-gluon plasma*, https://home.cern/science/physics/heavy-ions-and-quark-gluon-plasma, accessed: 2020-09-23

[5] K.C. Zapp, Eur. Phys. J. C **74**, 2762 (2014), 1311.0048

[6] A. Sirunyan, A. Tumasyan, W. Adam, E. Asilar, T. Bergauer, J. Brandstetter, E. Brondolin, M. Dragicevic, J. Erö, M. Flechl et al., Physical Review Letters **119** (2017)

[7] C. Andres, N. Armesto, H. Niemi, R. Paatelainen, C.A. Salgado, Phys. Lett. B **803**, 135318 (2020), 1902.03231